Icarus **148**, 52–64 (2000)
doi:10.1006/icar.2000.6484, available online at http://www.idealibrary.com on IDEAL®

Heliospheric Latitude Variations of Properties of Cometary Plasma Tails: A Test of the Ulysses Comet Watch Paradigm

John C. Brandt

Laboratory for Atmospheric and Space Physics, University of Colorado, Boulder, Colorado 80309, and Institute for Astrophysics, Department of Physics and Astronomy, University of New Mexico Albuquerque, New Mexico 87131
E-mail: jbrandt@as.unm.edu

and

Martin Snow

Laboratory for Atmospheric and Space Physics, University of Colorado, Boulder, Colorado 80309

Received September 29, 1999; revised February 7, 2000

Images of comets de Vico in 1995, Hyakutake in 1996, and Hale–Bopp in 1997 taken by observers in the Ulysses Comet Watch clearly show plasma tail properties reflecting the demarcation of the solar wind into distinct equatorial and polar regions with the boundary determined by the maximum extent of the heliospheric current sheet (HCS). Generally, (1) comet plasma tails in the polar region appear relatively undisturbed (as expected from a steady solar wind), while comet tails in the equatorial region appear disturbed (as expected from a highly varying solar wind); (2) disconnection events (DEs) are observed only in the equatorial region where comets pierce the HCS; (3) the position angle of the plasma tail is consistent with a solar wind speed of 750 km s^{-1} in the polar region and an average solar wind speed of 450 km s^{-1} in the equatorial region. While the paradigm seems firm, it was established during a limited range of the solar cycle, and an extension to other ranges is desirable.

We test this paradigm using the published record for essentially the entire 20th century. The catalogs of M. J. S. Belton and J. C. Brandt (1966, *Astrophys. J. Suppl.* 13, 125–332)—giving comet tail orientations and descriptive data—and M. B. Niedner (1981, *Astrophys. J. Suppl.* 46, 141–157)—giving DE data—were the principal sources. When combined with the DEs in Comet Halley (J. C. Brandt *et al.* 1999, *Icarus* 137, 69–83) and the Ulysses-era comets, the data set is extensive.

Results for the test are as follows:

(1) Images of Comet Mrkos (1957d) clearly show the change of appearance from polar to equatorial regions. We discuss the unusual case of Comet Borrelly (1903c) and present an evaluation of the descriptive notes in the Belton and Brandt catalog.

(2) The observed latitude envelope of DEs as a function of solar cycle is consistent with the maximum extent of the HCS. The HCS extends to higher latitudes at solar maximum (cf. J. T. Hoeksema 1991, *Adv. Space Res.* 11, (1)15–(1)24; S. T. Suess 1993, *Adv. Space Res.* 13, (9)31–(9)42) and the observed DEs trace this extension.

(3) The orientations of the plasma tail can be used to infer the solar-wind speed. Most of the suitable comets in the Belton and Brandt catalog are in the equatorial region, one is in the polar region, and a few cross the equatorial–polar boundary. In all cases, the orientation is consistent with a high-speed solar wind in the polar region and a lower-speed, variable solar wind in the equatorial region.

The data available for comets throughout the 20th century are consistent with the Ulysses Comet Watch paradigm. Thus, detailed studies of plasma tails can be used to map the structure of the heliosphere, specifically the location of the HCS and the location of the boundary between the equatorial and the polar regions. We note that data for comets in the polar region are still relatively rare.

Key Words: comets; solar wind.

1. INTRODUCTION

The ESA/NASA spacecraft Ulysses was launched in October 1990 to study many properties of the heliosphere. After a close encounter with Jupiter in February 1992 (Smith and Wenzel 1993), Ulysses was in an orbit with an inclination of 78.4° to the plane of the ecliptic. The orbital inclination to the solar equator was 80.2°, and the spacecraft would spend approximately 9 solar rotations above 70° heliographic latitude during its first revolution. The spacecraft and its orbit are well suited to study the properties of the solar wind as a function of latitude (Wenzel *et al.* 1992).

The belief that the near-equatorial region of the solar wind was not representative of the solar wind at higher latitudes was soon confirmed (Smith *et al.* 1995, Marsden *et al.* 1996). Basically, the heliosphere at roughly 1 AU heliocentric distance could be divided into two distinct regions (Phillips *et al.* 1995a,b). In the *polar region* the radial solar-wind speed W_r is approximately 750 km s^{-1} and the density $N_e = N_p = 3$ cm^{-3}. Variations in

0019-1035/00 $35.00

these properties are small. In particular, the heliospheric current sheet (HCS) does not extend into the polar region. In the *equatorial region*, the average radial solar-wind speed is 450 km s^{-1} and the average density is 9 cm^{-3}. Variations in these properties can be large. The equatorial region contains the HCS. The boundary between the polar and equatorial regions changes with the phase of the solar cycle and is determined by the maximum latitudinal extent of the HCS. A summary of the Ulysses solar-wind results is given in Fig. 1 (McComas *et al.* 1998).

2. THE PARADIGM

Comets are nature's *in situ* solar wind probes. Radiation from the Sun sublimates the icy material of the comet nucleus, some of which is then ionized. These ions are trapped by the Sun's extended magnetic field and form the plasma tail. Changes in the magnetic field structure and orientation are traced by the cometary plasma and can be observed from Earth. Interpretation of the large-scale morphology can help to understand the structure of the solar wind and the interplanetary magnetic field (IMF).

As part of the Ulysses program, J. C. Brandt was selected as an Interdisciplinary Scientist to explore the cometary implications of any latitudinal structure, including the possibility of using the properties of plasma tails as probes.

To secure an adequate data base of cometary images, the Ulysses Comet Watch (UCW) was established consisting of observers around the world who agreed to supply images. Communication with the UCW was carried out via the *UCW Newsletter* (14 issues from February 10, 1993, to August 1, 1998).

The expectations, based on the paradigm, were as follows.

(1) *Appearance.* Comet tails in the polar region should appear relatively undisturbed because they are exposed to a steady solar wind. Tails in the equatorial region should appear disturbed because they are generally exposed to a highly varying solar wind.

(2) *Disconnection Events (DEs).* The generally accepted view of DEs is that they occur when a comet pierces the HCS (Niedner and Brandt 1978, Niedner and Schwingenshuh 1987, Delva *et al.* 1991, Yi *et al.* 1994, 1996, 1998, Voelske and Matsuura 1998, Brandt *et al.* 1999), but the acceptance is not universal (Saito *et al.* 1987, Farnham and Meech 1994, Wegmann 1998). In the generally accepted view, DEs should be observed in the equatorial region but not in the polar region.

(3) *Orientation of Plasma Tail.* The solar-wind speed determines the orientation of the plasma tail (Biermann 1951, Brandt *et al.* 1972). Thus, the orientation of plasma tails in the polar region should correspond to the 750 km s^{-1} solar-wind speed and have a small spread around the average. Comets in the equatorial region should have an orientation corresponding to 450 km s^{-1} and have a large spread around the average. The general pattern is a high-speed regime (polar) with small scatter versus a lower speed regime (equatorial) with higher scatter.

The paradigm is illustrated schematically in Fig. 2.

Although some elements had certainly been proposed earlier, the comet/solar-wind paradigm was clearly recognized during the Ulysses Comet Watch (Brandt *et al.* 1998). This came about because three comets with high inclinations became available and the recent cometary results could be combined with the measurements from Ulysses. These were comets de Vico (C/122P) in 1995 ($i = 85.4°$), Hyakutake (C/1996 B2) in 1996 ($i = 124.9°$), and Hale–Bopp (C/1995 O1) in 1997 ($i = 89.4°$). Each of these comets was transregional; i.e., they passed across the boundary between the polar and equatorial solar-wind regions, and two of them were bright. We now understand that such crossings are rarely observed events.

The detailed reports for these comets have been published (Brandt *et al.* 1997) or are in preparation (Snow, Brandt, Yi, Peterson, and Mikuz, Comet Hyakutake (C/1996 B2) and the latitudinal structure of the solar wind, in preparation; Brandt, Snow, Yi, Larson, Mikuz, Peterson, and Liller, Large-Scale structures in Comet Hale–Bopp (C/1995 O1): Latitudinal variations and monster disconnection event, in preparation). We illustrate the results from these three comets as a guide to following the main tests presented in this paper.

The change in appearance is best seen with a daily (or more frequent) image sequence taken with the same telescope. Figure 3 shows such a sequence for comet Hyakutake in April 1996 taken by H. Mikuz at the Crni Vrh Observatory, Solvenia (Snow, Brandt, Yi, Peterson, and Mikuz, Comet Hyakutake (C/1996 B2) and the latitudinal structure of the solar wind, in preparation). The HCS extended to approximately 30°N latitude. Notice in Fig. 3 that the tail appearance is much more disturbed for the images of April 18.8 and earlier, corresponding to latitudes of 30.1° and lower, than for the images of April 19.9 and later, corresponding to latitudes of 32.4° and higher. Similar behavior was seen in comets de Vico and Hale–Bopp.

All three comets displayed one or more *disconnection events*. All comets were close to the HCS at the time of the DEs and well within the equatorial region.

Comet de Vico clearly showed the change in plasma tail orientation expected. In Fig. 4 (from Brandt *et al.* 1997), we show the orientation (via the position angle) of the plasma tail versus date. The boundary between the polar and equatorial regions is marked by the gray bands centered on 20° latitude (north and south). The curves for $W_r = \infty$ (the PRV, prolonged radius vector), $W_r = 750$ km s^{-1}, and $W_r = 450$ km s^{-1} are shown. The points fall near the 750 km s^{-1} curve and have a small scatter for the polar region. In the equatorial region, the points fall near the 450 km s^{-1} curve and have a larger scatter.

The comparison shown for comet de Vico was carried out assuming that the solar wind flow was strictly radial, i.e., assuming that the nonradial components, W_ϕ and W_θ, were zero. These can produce significant effects on the tail position angles depending on the geometrical circumstances. However, the general pattern remains—a higher speed regime with small scatter versus a lower speed regime with higher scatter.

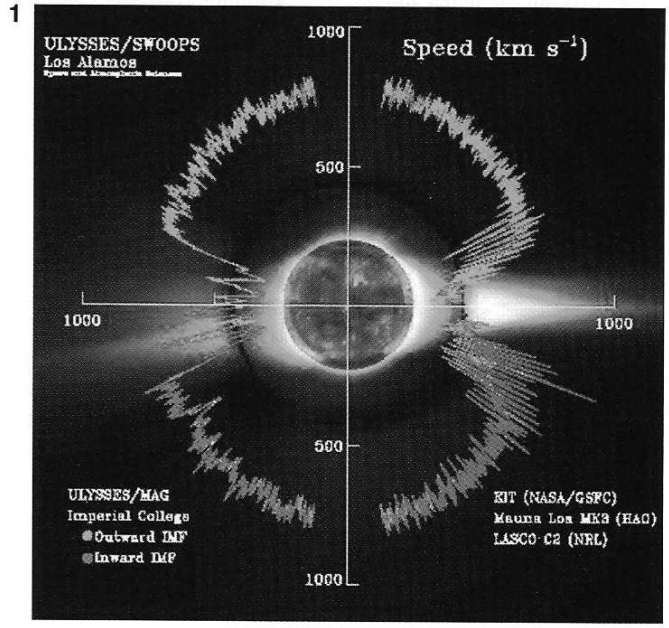

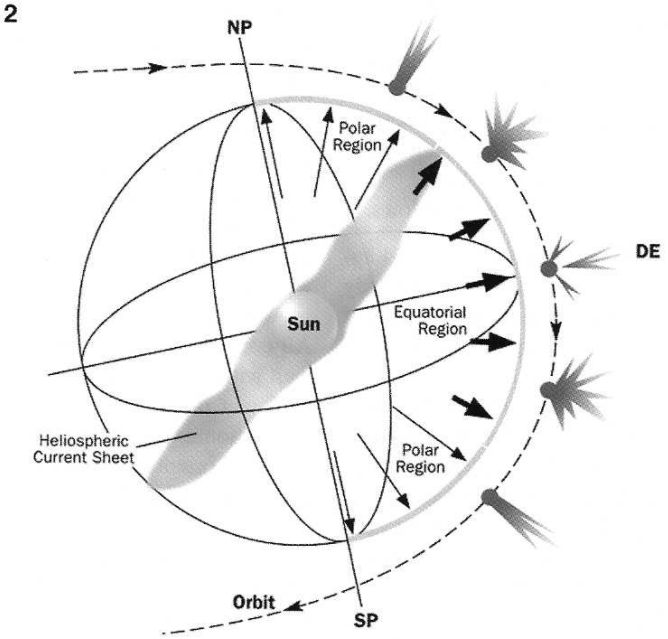

FIG. 1. A polar plot of Ulysses/SWOOPS solar-wind speeds with additional information as noted. The solar-wind speed of 750 km s^{-1} with small variations at high latitudes and the solar-wind speed of 450 km s^{-1} with large variations at low latitudes is clearly shown (from the Ulysses webpage, http://swoops.lanl.gov and McComas *et al.* 1998. Courtesy of David McComas, Southwest Research Institute).

FIG. 2. Cartoon of the paradigm. In the polar region, the long, thin arrows show the high-speed, low-density solar wind, while in the equatorial region, the short, thick arrows show the low-speed, high-density solar wind. The relatively constant speed in the polar region produces an undisturbed plasma tail, while the highly variable speed in the equatorial region produces a disturbed plasma tail. DEs occur only in the equatorial region. The boundary between the polar and the equatorial regions is the maximum extent of the heliospheric current sheet (HCS), a tilted wavy sheet shown here foreshortened. The HCS rotates with the Sun.

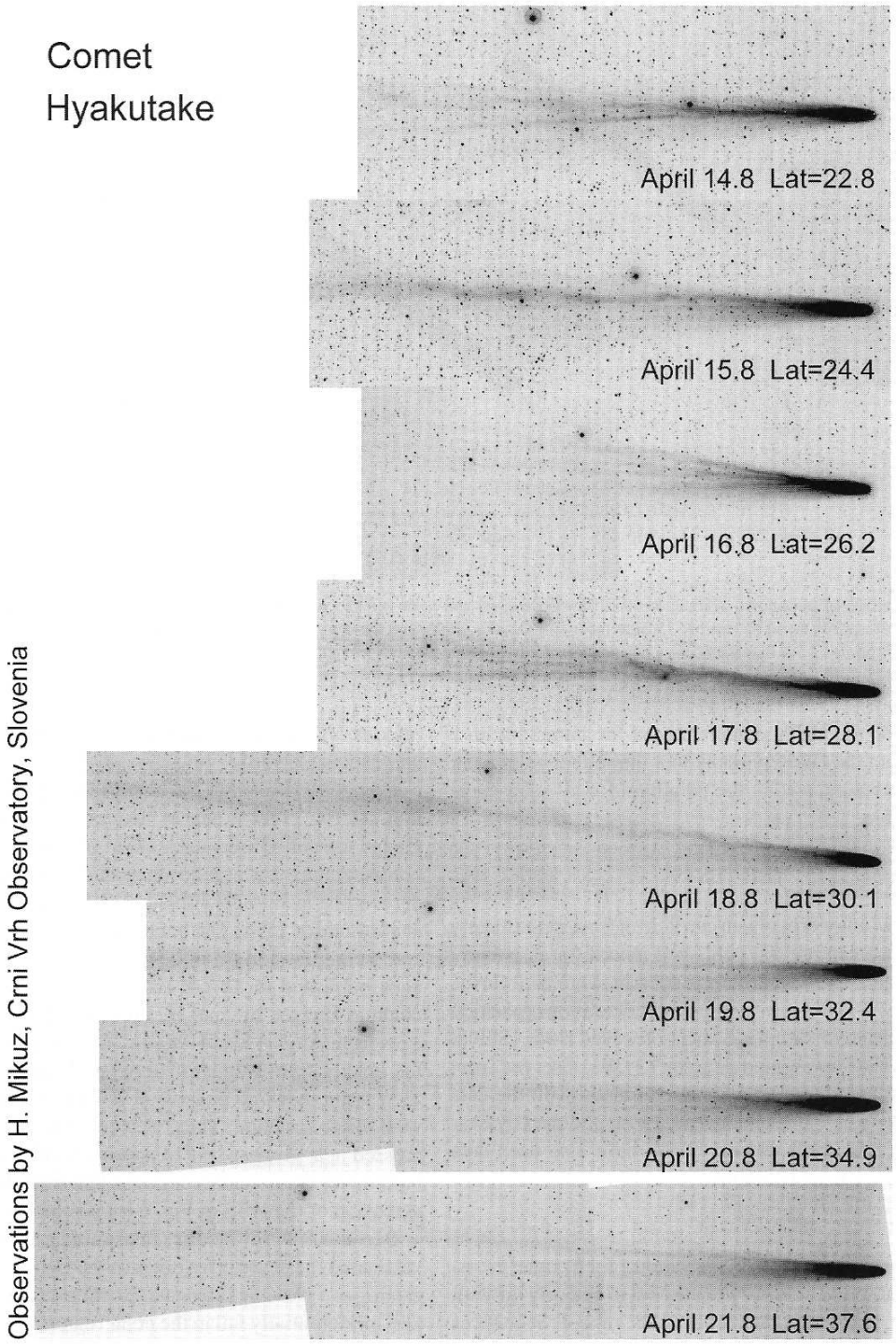

FIG. 3. Sequence of images of Comet Hyakutake taken by H. Mikuz, Crni Vrh Observatory, Slovenia. The dates and latitudes are marked. The boundary was located at about 30°N. The comet has a relatively disturbed appearance at lower latitudes are relatively smooth appearance at higher latitudes. (Snow, Brandt, Yi, Peterson, and Mikuz, Comet Hyakutake (C/1996 B2) and the latitudinal structure of the solar wind, in preparation).

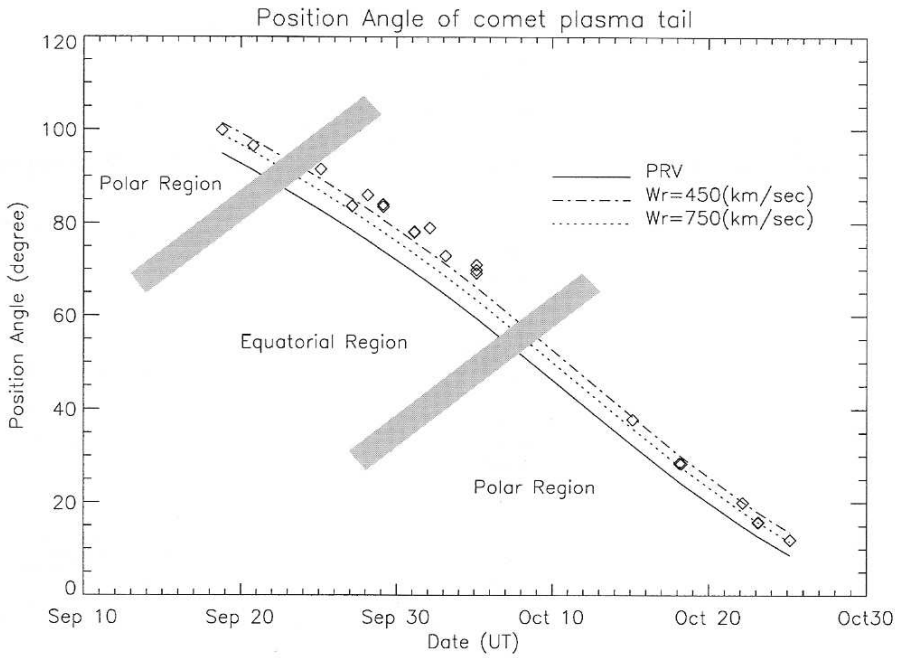

FIG. 4. Comparison of plasma-tail orientations (via position angles) and solar-wind speeds for the equatorial and polar regions for Comet de Vico. The equatorial region corresponds to approximately 25 September to 9 October, 1995, and the boundary is marked with the two gray bands centered on 20° latitude (north and south) (Reprinted from Planetary Space Science Vol. 45, by Brandt, Yi, Petersen, and Snow, Comet de Vico (122 P) and latitude variations of plasma phenomena, pages 813–819, Copyright 1997, with permission from Elsevier Science).

The results for the UCW comets placed the paradigm on a sound footing, but they strictly apply to a limited range of solar cycle phase. Therefore, testing the paradigm for all solar-cycle phases is desirable.

3. THE TESTS

Photography of comets has been carried out for approximately 100 years, and we can use the published record for essentially the entire 20th century. The principal sources were as follows. Belton and Brandt (1966) gave comet–tail orientations (position angles) and descriptive data for comets observed from 1889 to 1963. Niedner (1981) presented data for 72 DEs observed from 1892 to 1976. When these sources are combined with the data for DEs in Halley's comet (Brandt *et al.* 1999) and the Ulysses-era comets, the data set is extensive. We have also used data from the literature where available.

3a. Appearance

The search for clear changes in appearance for a comet crossing the equatorial–polar boundary turned out to be fairly difficult for two reasons. The first is the nature of the record. Sequences such as the one shown in Fig. 3 for Comet Hyakutake are rare in the older record. Also, the exposure times were often quite long (which complicates the interpretation, see below) and many plates are unpublished in observatory vaults. The second is that the record shows only three comets prior to 1960 that were well-observed in both the equatorial and the polar solar-wind regions. These were comets Borrelly (1903c), Brooks (1911c), and Mrkos (1957d).

Comet Mrkos shows the change in appearance at the boundary; see Fig. 5 for a pair of images kindly supplied by Henry Giclas, Lowell Observatory taken on August 15 and 21, 1957, corresponding to a latitude range of 73°N to 54°N (the comet was descending in latitude with time). A DE took place on August 22 at a latitude of 53°N. The boundary crossing can be pinned down and the impression from the images in Fig. 5 confirmed by images published in *Sky & Telescope*. The October 1957 issue contains images by Paul H. Preo and Alan McClure. The images from August 8 and August 16 are relatively smooth, while the images from August 17 through 22 are not. The December 1957 issue shows an image by Choko Fujita on August 23, 1957 with major structure. Thus, we conclude that the boundary was crossed near August 16.5 at approximately 65°N latitude. This latitude for the boundary is consistent with the adopted latitude extension of the HCS in Fig. 6 for a solar cycle phase of 0.32.

Because of the difficulties in obtaining suitable images, we investigated the descriptive notes in the Belton and Brandt (1966) catalog as a possible surrogate. Do the points for "smooth tail image" preferentially fall in the polar region? Do the points labeled "tail shows turbulent structure," "condensations in tail," and "sharp discontinuity in tail" preferentially fall in the equatorial region? Where these descriptive notes are given, we have plotted them for all the comets in Table I and see no believable trend.

A brief discussion of the Belton and Brandt (1966) descriptive notes is in order. The goal of the 1966 paper was to assemble

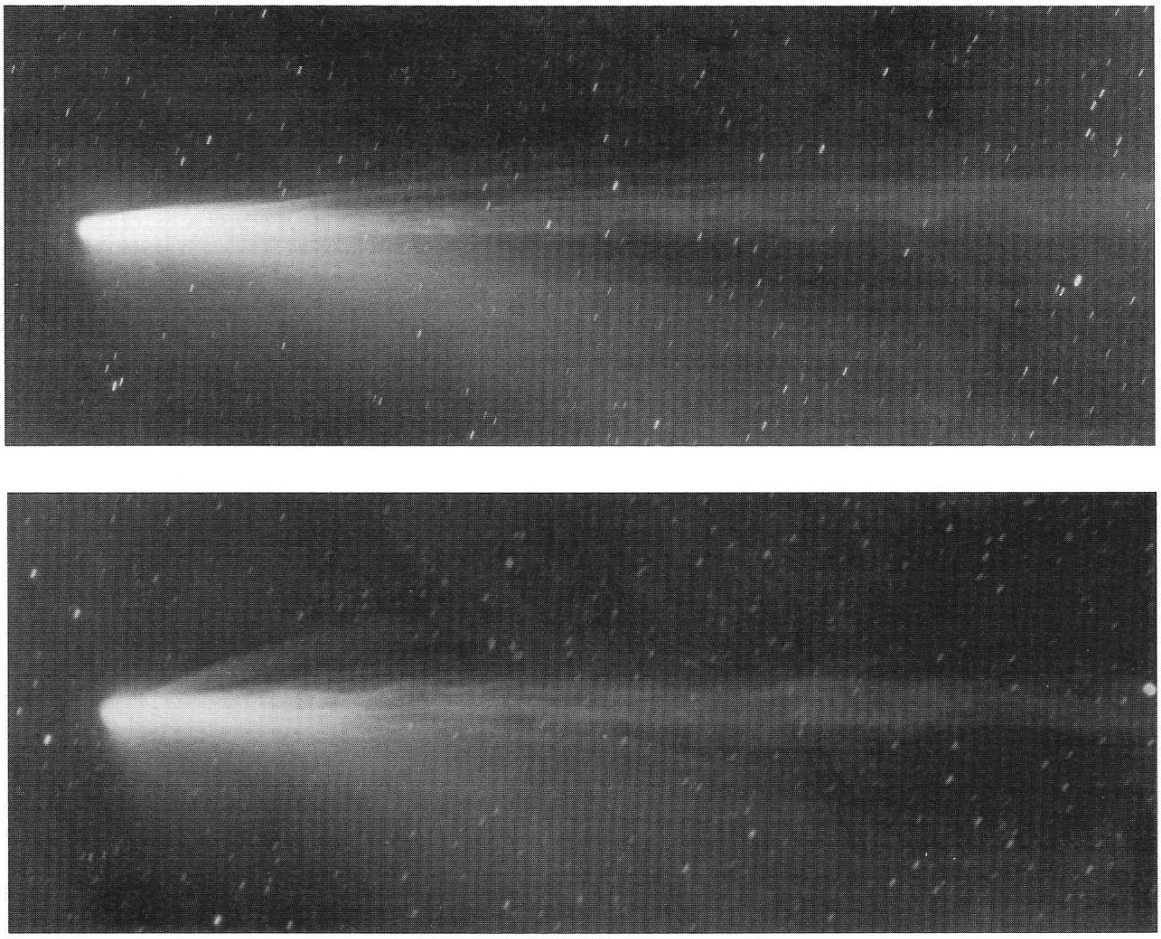

FIG. 5. Images of Comet Mrkos (1957d) showing the transition from a polar-region comet to an equatorial-region comet. (Top) August 15, 1957, with a relatively undisturbed appearance at 73°N. (Bottom) August 21, 1957, with a disturbed appearance at 54°N. See text for discussion (courtesy of Henry Giclas, Lowell Observatory).

a data base of reliable comet–tail orientations. The descriptive notes were not a high-priority item and they were not given at all for many observations in the catalog. We illustrate some of the problems in using the notes, e.g., different exposure times and differing ideas of "disturbed" in the next paragraph. The basic distinction that needs to be made is "absolute" disturbed structure vs "relative" disturbed structure. When a homogeneous sequence of images is available as in the case of Comet Hyakutake (Fig. 3), the relative change in disturbed appearance is easy to see. Assigning an index for disturbed appearance on an absolute scale is not easy and may well be impossible.

The case of Comet Borrelly (1903c) is instructive. Essentially, the opposite behavior was found; i.e., the tail was described (by Belton and Brandt 1966) as "smooth" at equatorial latitudes (including exposures covering the clearly visible DE of July 24.6, 1903) and no descriptors given at polar latitudes. The comet was in the equatorial region from June 23 to July 29, 1903, and moved from latitude 7°N to 30°N. The comet was in the polar region from August 11 to August 18, 1903, and moved from latitude 52°N to 77°N. These are the time intervals covered by observations in the Belton and Brandt catalog. The demarkation is consistent with our adopted HCS. While moving in latitude, the comet was also moving towards perihelion. Its heliocentric distance was 1.53 AU on June 22 and 0.42 AU on August 18. The situation from the observer's viewpoint was summarized in *The Lick Observatory Bulletin* (Albrecht 1904)

> There is a marked contrast in the appearance of the primary tail on the negatives taken in July and on those taken in August. The tail on the plates of July is, with three exceptions [Note: the DE mentioned above] ... smooth and continuous, while on the August plates it is twisted and full of condensations, indicating greatly increased activity as the comet approached perihelion.

The main culprit is probably the exposure time, 3 h on July 1 and 1 h on August 15. These exposure times are representative and reflect the brightening of the comet as it approaches perihelion. Structure would be smeared out on the longer exposures yet

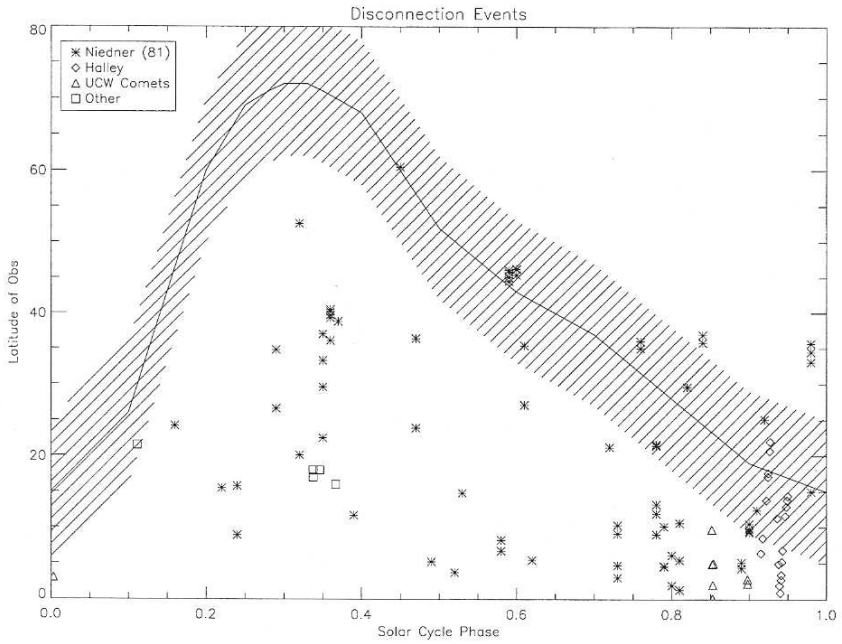

FIG. 6. The latitudes of 100 observed DEs versus solar-cycle phase. Solar minimum is at 0.0 and 1.0, solar maximum is at 0.4. The nominal maximum extension of the HCS is plotted as the solid line; see text for discussion and the comets included in "Other." The upper envelope for DEs traces the change of the HCS maximum latitude.

visible on the shorter ones. The reported differences were not likely to have been intrinsic to the comet. Another factor is the evolution of our knowledge of comets. The images showing the DE would be considered disturbed now, but were not circa 1965.

Where the images are available and reasonably modern, i.e., Comet Mrkos in 1957, they show the change in appearance expected. Caution, however, should be used when using older images. The descriptors in the Belton and Brandt (1966) catalog are not reliable surrogates for the appearance changes described in this paper. The best approach is to use a homogeneous sequence of images, e.g., the images of comet Hyakutake shown in Fig. 3.

3b. Disconnection Events

Figure 6 shows a plot of DE latitude versus solar-cycle phase for 100 DEs. The DEs consist of 72 from Niedner's (1981) catalog, 19 from Comet Halley (Brandt *et al.* 1999), 4 from the UCW comets (2 probables from Comet de Vico and one each from comets Hyakutake and Hale–Bopp), and 5 additional from the literature. The latter are one possible DE in Comet Bradfield (1979X) (Schulz *et al.* 1994), one DE in Comet Bradfield (1987s) (Cremonese and Fulle 1988), two possible DEs in Comet Austin (1990V) (Farnham and Meech 1994), and one DE in Comet Levy (1990c) (Kosuka *et al.* 1991). These are plotted as "Other" in Fig. 6.

The observed latitude envelope of DEs as a function of phase of the solar cycle is generally consistent with the predicted extent of the HCS. We have adopted a nominal curve for the HCS, the solid line in Fig. 6, based on data taken from Hoeksema (1991) and Suess (1993), and have roughly indicated the typical variations with hatching. The tilt angle of the HCS to the solar equator is the same as the maximum excursion of the HCS in solar latitude. The calculated heliospheric current sheet position is based on photospheric magnetic field measurements. From these, a potential field model is used to calculate the field on a coronal source surface, usually taken to be a sphere with radius 2.5 Rs. A radial projection of the field on the source surface gives the calculated HCS location throughout the heliosphere.

The HCS extends to higher latitudes at solar maximum and the DEs trace this extension. Of the 100 DEs plotted, 95 are in the average equatorial region, 2 are just outside the hatched area, and 3 are approximately 10° above the hatched area. The 2 just oustide the hatched area near $P = 0.84$ are Comet Brooks (1911c) in September 1911. These points are not a problem for the latitude envelope of DEs, but require discussion (below) in terms of the plasma tail orientations. The three points some 10° outside the hatched area near $P = 0.98$ are Comet West (1975n) in March of 1976 (Niedner 1981; see Plate 1). Niedner (1982) noted that 2 of the 3 DEs in Comet West "... form reasonably close associations with corotated sector boundaries ..." and pointed out that the principal uncertainty was, of course, the latitude of 35°. Fluctuations in latitude of order 10° from the mean HCS location for a given solar cycle are common and we conclude that the points for Comet West are consistent with the paradigm, along with the rest of the DE data.

TABLE I
Comets in the Belton-Brandt Catalog Suitable for Plasma Tail Orientation Studies

Comet	Latitude range (°)	Approximate maximum latitude of nominal HCS (°)	Comments
Swift (1892a)	14N–45N	63	Equatorial
Rordame–Quenisset (1893a)	20N	72	Equatorial
Brooks (1893d)	21N–40N	71	Equatorial
Gale (1894b)	18S–7S	68	Equatorial
Perrine (1898b)	60N–78N	36	Polar
Swift (1899a)	35N–25N	28	Equatorial
Perrine–Borrelly (1902b)	17N–30N	26	Equatorial
Borrelly (1903c)	7N–77N	43	Transregional, poor geometry
Giacobini (1905c)	35N–37N	70	Equatorial
Daniel (1907d)	5N–9S	53	Equatorial, poor geometry
Morehouse (1908c)	46N–43S	43	Equatorial, poor geometry
Kiess (1911b)	30N–11N	27	Equatorial
Brooks (1911c)	35N–5S	23	Transregional
Peltier (1936a)	2N–23S	69	Equatorial
Finsler (1937f)	40N–25N	70	Equatorial
Jurlof–Achmarof–Hassel (1939d)	27N–6N	51	Equatorial
Cunningham (1940c)	51N–48N	38	Only 3 points, 2 look equatorial
Whipple–Fedtke–Tevadze (1942g)	0–13N	19	Equatorial
Abell (1953g)	36N–11S	15	Only 3 points, equatorial
Mrkos (1957d)	76N–20N	72	Transregional

We elaborate on the last statement by discussing sources of uncertainty in the calculated HCS position. The hatched area in Fig. 6 is intended to show the uncertainty from fluctuations smoothed out in the calculations and variations from one solar cycle to the next. Structure and/or fluctuations in the HCS have been discussed in the literature for years (e.g., Behannon *et al.* 1981, Crooker *et al.* 1993, Burton *et al.* 1994, Suess *et al.* 1995). The cause can be coronal mass ejections (CMEs), shears in the solar-wind flow, solar-wind eddies, waves, or structure that results in multiple current sheets. The possibilities are substantial, but it is difficult to be quantitative for specific cases. In the study of the 19 DEs in Halley's comet (Brandt *et al.* 1999), the good knowledge of the calculated HCS from December 1985 to May 1986 and 48 spacecraft crossings provided an opportunity for quantitative results. The fit to the HCS was optimized to minimize the rms dispersion for spacecraft crossings which was 5.2°. The rms dispersion for DE positions relative to the calculated HCS was 8.2° to 10.9°, depending on the details. The dispersion for DEs is larger than the dispersion for spacecraft because of the uncertainty in the time between the HCS encountering the comet and the onset of the DE. Given this level of dispersion when the HCS is well determined, we do not find a small number of observations on the wings of the distribution (for the DEs in Comet West, this corresponds to about 20° from the mean HCS position or about 10° from the edge of the hatched area in Fig. 6) to be unusual or a source of concern. Finally, we feel that sometimes the exact location of the calculated HCS is taken too seriously.

We briefly discuss Niedner's (1982) paper that presaged the DE part of the paradigm. His Fig. 7 was an earlier version of our Fig. 6. Only 41 DEs were used in the earlier figure because the sample was restricted to those DEs produced by sector boundaries that intercepted Earth. Niedner concluded that the latitudinal distribution of DEs over solar cycle phase was reasonably consistent with estimates of the maximum latitudinal extent of the HCS. Recall that the maximum extent in latitude of the HCS was not well understood at the time. Niedner's conclusion rested on the assumption that DEs are caused by magnetic reconnection at crossings of the HCS. This assumption and the existence of a small number of high latitude DEs lead Niedner also to conclude that the HCS can extend to latitudes of 45° or higher. The general understanding of the location of the HCS during the solar cycle, the Ulysses measurements, and our results with a larger sample of DEs confirm Niedner's (1982) conclusions.

3c. Plasma Tail Orientations

Belton and Brandt (1966) assembled a catalog of cometary observations spanning most of the modern era of photographic plates. They tabulated tail orientations for 1607 observations, of both plasma and dust tails. Of course, we are interested in only Type I or plasma tails. Position angles are not reliable for situations where the dust and plasma tails were difficult to distinguish on the plates; this rules out comets Halley (1909c) and Arend-Roland (1956h). Also, Belton and Brandt noted systematic differences between visual and photographic position angles and therefore the visual observations of M. Beyer are not used. Finally, a handful of individual observations were rejected. The arguments are the same as given by Brandt *et al.* (1972, Appendix B), but the reference to comet "1906c" is spurious.

The plasma tail orientations listed in the Belton and Brandt catalog have been analyzed to determine the solar-wind speed (Brandt *et al.* 1972) and these results give a good idea of the mean speed in the equatorial region as derived from comet–tail orientations. While the measurements were of equatorial and polar comets, there were only about 58 polar observations in the total sample of 700. Thus, the sample is overwhelmingly equatorial. The results for the mean solar wind were $W_r = 415 \pm 13$ km s^{-1}, low values for the mean azimuthal and meridional components, and a peculiar, isotropic velocity of about 40 km/s.

Only comets with three or more observations are considered here. The sample available is listed in Table I, where each comet is classified by region. The classification is a judgement based on consistency of the orientation and the mean HCS curve in

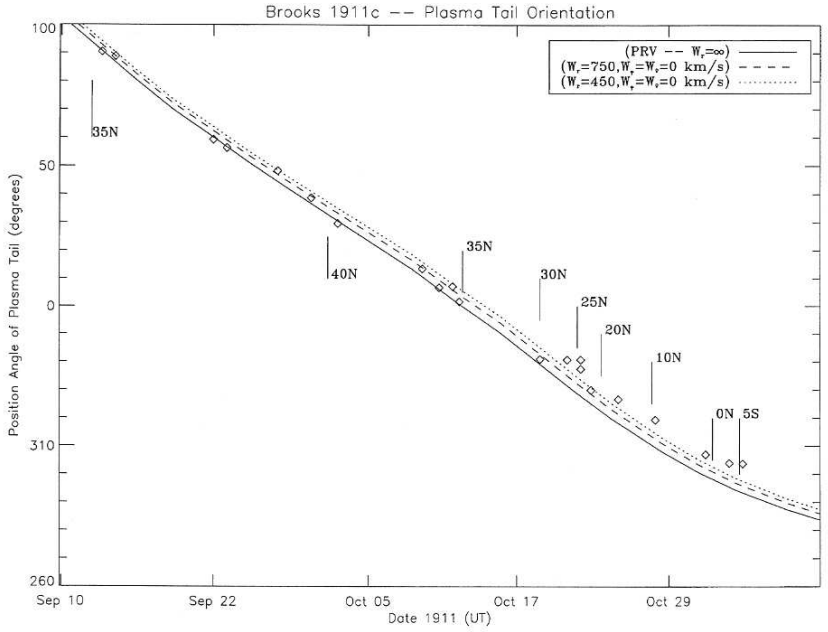

FIG. 7. Comparison of plasma-tail orientations versus time for the transregional Comet Brooks (1911c) and reference curves for different solar-wind speeds (see Fig. 4 and discussion in the text). The boundary is at approximately 28°N latitude on October 20, 1911; see text for discussion. The latitude of the comet is marked. The degree symbol for the latitudes has been dropped to avoid clutter in Figs. 7 through 11.

Fig. 6. The mean HCS curve was used to determine the maximum latitude of the HCS listed in Table I. Belton and Brandt compared multiple measurements of orientations (position angles) to assign a deviation around the mean of 1.5°. The comparisons were made on dust tails. The deviation for plasma tails should be smaller and a useful value is 1.0°.

For the 20 comets available, one has three observations in the polar region (Perrine 1898b), three are transregional (Borrelly

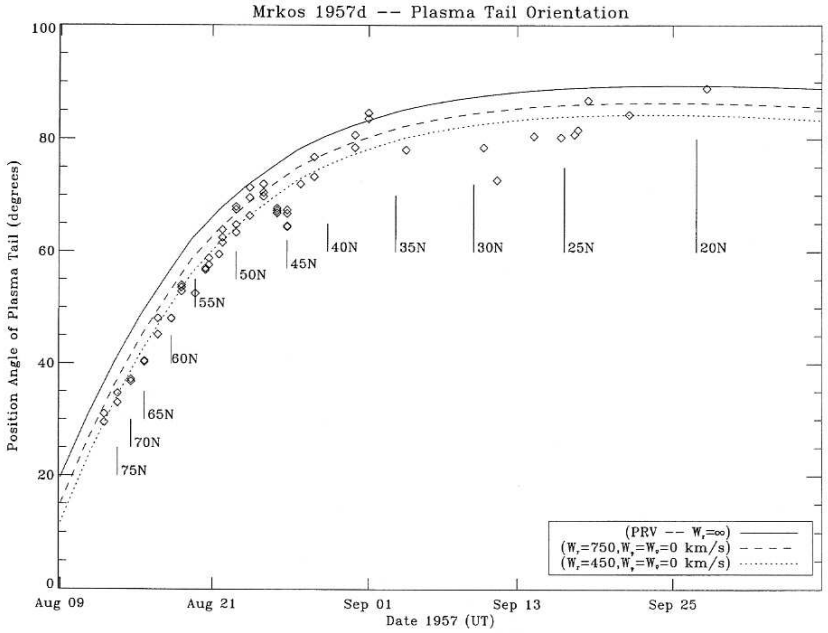

FIG. 8. Comparison of plasma-tail orientations versus time for the transregional Comet Mrkos (1957d) and reference curves for different solar-wind speeds. See text for discussion of this comet and determination of the boundary at approximately 65°N on August 16.5, 1957. The latitude of the comet is marked.

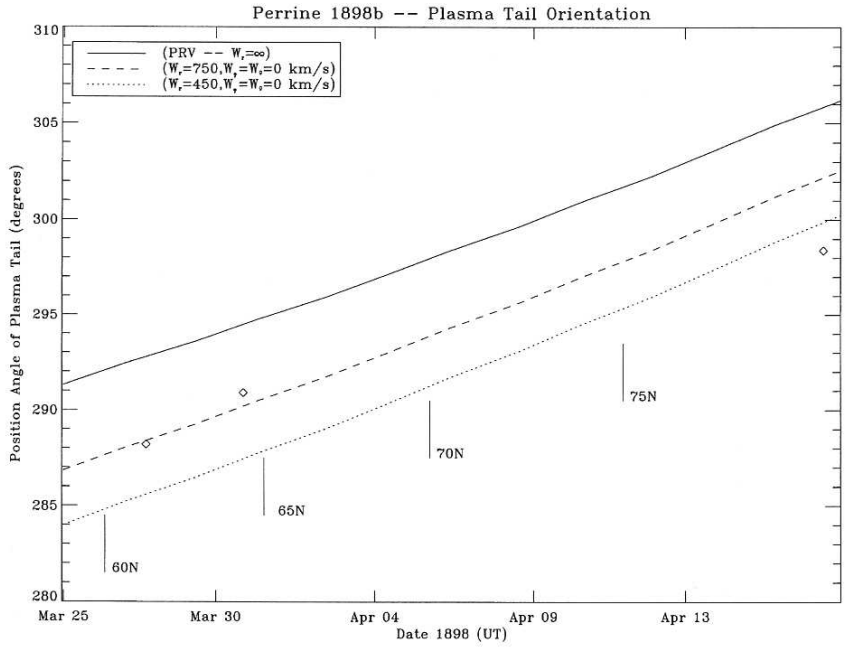

FIG. 9. Plasma-tail orientations for the polar Comet Perrine (1898b). See text for discussion. The latitude of the comet is marked.

1903c, Brooks 1911c, and Mrkos 1957d), and 16 are equatorial or consistent with this assignment where there are a small number of measured tail position angles.

The transregional comets largely exhibit the behavior predicted by the paradigm. Figure 7 shows the plot of position angle versus time with the comparison curves for Comet Brooks. The comet shows a high-velocity, low-variability solar wind until approximately October 20 at 28°N. This is consistent with the adopted HCS latitude extension (Fig. 6). Then it exhibits the slower speed with higher variability. While the tail orientations

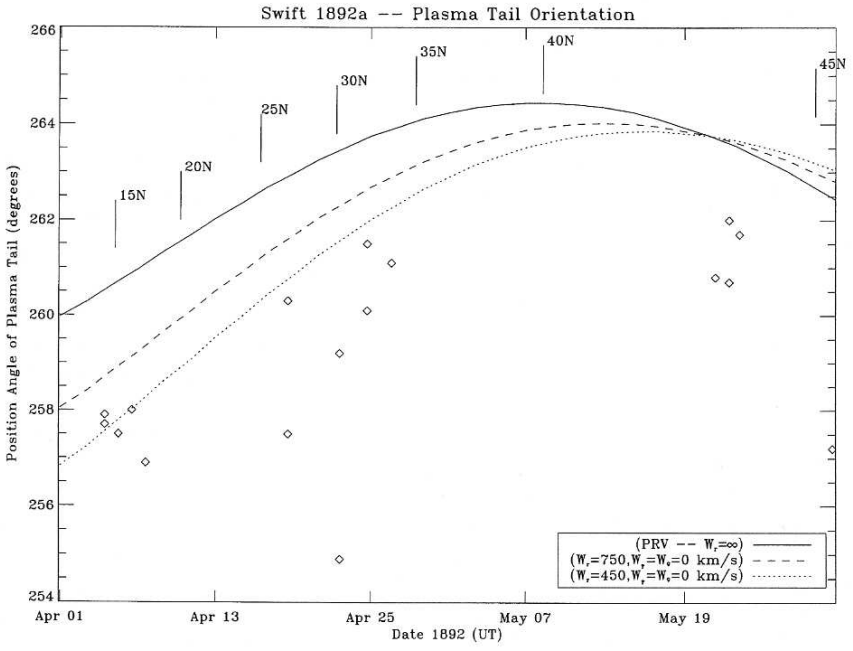

FIG. 10. Plasma-tail orientations for the equatorial comet Swift (1892a). The latitude of the comet is marked.

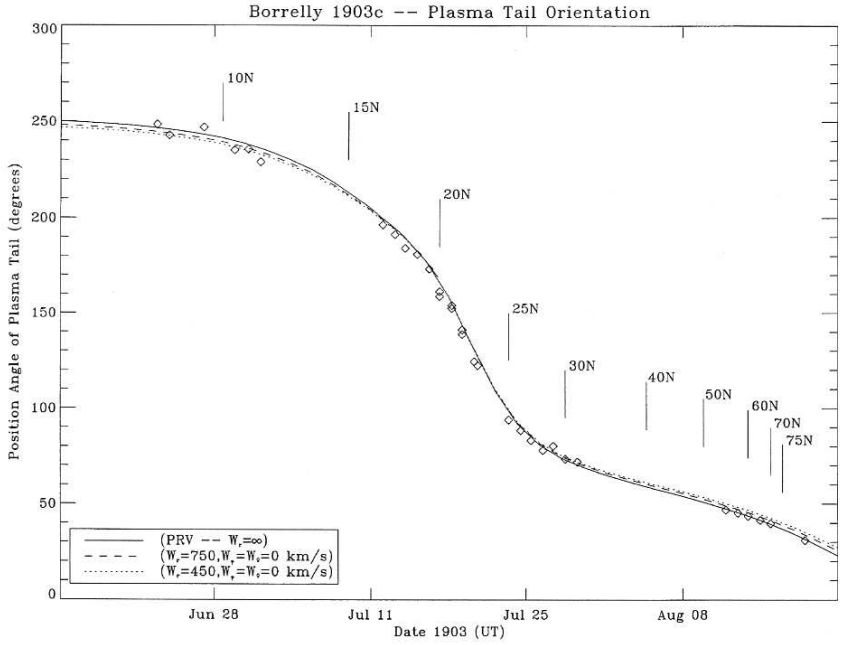

FIG. 11. Plasma-tail orientations for the transregional Comet Borrelly (1903c), showing the effects of poor geometry. The latitude of the comet is marked.

shown in Fig. 7 nicely fit the paradigm, we note that Niedner (1981) lists DEs in Comet Brooks on September 16.3 (at latitude 36°N) and 20.4 (at latitude 37°N), described as "certain" and "fairly certain," respectively. They could indicate an exception to the paradigm. Other possibilities are: (1) a disturbance temporarily moved the HCS to a higher latitude at the time of these DEs; (2) these events mimicked DE morphology, but were not DEs; or (3) a magnetic reversal not directly associated with the HCS (Niedner and Brandt 1979) produced these DEs. Basically, the data for the relevant time period are sparse and a definitive conclusion cannot be drawn.

Figure 8 shows the position angle plot for comet Mrkos. The comet was descending in latitude and shows the higher-speed, lower-scatter behavior until approximately August 16.5 at 65°N latitude. (This date is taken from the discussion of the images and is consistent with the position angle data). Then, the points show the lower speed and higher scatter.

Some of the comets have unfavorable geometry for this type of analysis. Unfortunately, one of these was our transregional comet, Borrelly 1903c (see below).

Figure 9 shows the position angle plot for Comet Perrine. Two of the points (at latitudes of 60° and 63°) fall close to the expected 750 km s^{-1} curve, but one point (April 17, 1898, at latitude 78°) does not. While a single point may not be significant, it may exhibit an anomalous position-angle behavior also seen in Comet Hale–Bopp at the highest latitudes (Brandt, Snow, Yi, Larson, Mikuz, Peterson, and Liller, Large-Scale structures in Comet Hale–Bopp (C/1995 O1): Latitudinal variations and monster disconnection event, in preparation).

Figure 10 shows the position angle plot for the equatorial Comet Swift (1892a). The data are representative of the slow-speed, variable solar-wind environment. The consistency of this interpretation for the other equatorial comets was checked directly in the Belton and Brandt catalog. The solar-wind speed assuming purely radial flow is tabulated and inspection shows that the classification of comets in Table I is consistent with the data.

For some of the comets of interest, the geometry is unfavorable and the curves for the different solar-wind speeds are essentially coincident. Figure 11 shows the plot for Comet Borrelly (1903c), one of the transregional comets. While the plot is consistent with the paradigm (the comet was in the polar region for the August 1903 observations), no firm conclusions can be drawn. We have done the plot for the famous Comet Morehouse (1908c), and it shows little more than poor geometry.

The plasma–tail orientation data in the Belton and Brandt catalog provide quantitative evidence for the paradigm. The data largely support the equatorial–polar picture.

4. CONCLUSIONS

Published cometary data for essentially the entire 20th century have been examined as a test of the demarcation of the heliosphere into equatorial and polar solar-wind regions. The limited number of modern images available for comets crossing the boundary (e.g., Comet Mrkos), the latitude distribution of 100 DEs as a function of solar-cycle phase, and the orientations of plasma tails (particularly for comets Brooks and Mrkos,

which crossed the boundary) support the UCW paradigm for plasma-tail behavior. The paradigm has been shown to apply for many years and essentially the entire solar cycle.

These kinds of plasma-tail studies can be used to map the structure of the heliosphere. The three elements of the paradigm—appearance of comets, locations of DE occurrence, and the position angles of plasma tails—can be used to infer the position of the HCS and the equatorial–polar region boundary. This independent approach could be quite useful in the future when we do not have direct measurements from Ulysses, the only spacecraft to date to explore the high-latitude heliosphere. Priority should be given to observations of comets likely to cross the equatorial–polar boundary. We may hope that such opportunities continue to arise. The best observational approach utilizes homogeneous sequences of wide-field images as shown in Fig. 3.

We know of only six comets—Borrelly (1903c), Brooks (1911c), Mrkos (1957d), de Vico (C/122P), Hyakutake (C/1996 B2), and Hale–Bopp (C/1995 O1)—that were observed while crossing the equatorial–polar boundary and only one—Comet Perrine (1898b)—with observations exclusively in the polar region. These facts serve to emphasize the extreme rarity of comets extensively observed while in the polar region.

The relative dearth of well-observed polar comets underscores the value of Comet Hale–Bopp as the exception. This large, bright comet with an orbit almost perpendicular to the plane of the ecliptic was very well observed for months in the polar region, particularly during March and most of April 1997. The comet's beautiful and ethereal appearance—the blue plasma tail with some filamentary fine structure, but very little gross structure—was due to the environment of the polar solar-wind region. This comet deserves an extensive discussion of the large-scale plasma structure, and that paper is in preparation (Brandt, Snow, Yi, Larson, Mikuz, Peterson, and Liller, Large-Scale structures in Comet Hale–Bopp (C/1995 O1): Latitudinal variations and monster disconnection event, in preparation).

ACKNOWLEDGMENTS

The paradigm discussed in this paper was made possible by the expert and generous cooperation of the Ulysses Comet Watch observers. We thank them again. We thank the director and staff of the Lowell Observatory for their hospitality in making their Library available to us. We thank Dr. Henry Giclas, Lowell Observatory, for supplying the images of comet Mrkos. We thank Dr. David McComas, Southwest Research Institute, for permission to use Figure 1 summarizing the *Ulysses* results. We also thank the referees, Dr. Tony Farnham and Dr. Malcolm B. Niedner, Jr., for valuable comments. This research was supported by JPL Grant 959349 to John C. Brandt as an Interdisciplinary Scientist on the *Ulysses* Project.

REFERENCES

Albrecht, S. 1904. Photographic observations of Comet 1903 c (Borrelly). *Lick. Obs. Bull.* **2**, 163–168.

Behannon, K. W., F. M. Neubauer, and H. Barnstorf 1981. Fine-scale characteristics of interplanetary sector boundaries. *J. Geophys. Res.* **86**, 3273–3287.

Belton, M. J. S., and J. C. Brandt 1966. Interplanetary gas. XIII. A catalogue of comet-tail orientations. *Astrophys. J. Suppl.* **13**, 125–332.

Biermann, L. 1951. Kometenschweife und solar korpuskularstrahlung. *Z. Astrophys.* **29**, 279–286.

Brandt, J. C., F. M. Caputo, J. T. Hoeksema, M. B. Niedner, Jr., Y. Yi, and M. Snow 1999. Disconnection events (DEs) in Halley's comet 1985–1986: The correlation with crossings of the heliospheric current sheet (HCS). *Icarus* **137**, 69–83.

Brandt, J. C., C. C. Petersen, M. Snow, Y. Yi, and the Ulysses Comet Watch 1998. Cometary plasma tails as probes of latitudinal structure in the solar wind. *Ann. Geophys.* **16** (Suppl. III), C859.

Brandt, J. C., R. G. Roosen, and R. S. Harrington 1972. Interplanetary gas. XVII. An astrometric determination of solar-wind velocities from orientations of ionic comet tails. *Astrophys. J.* **177**, 277–284.

Brandt, J. C., Y. Yi, C. C. Petersen, and M. Snow 1997. Comet de Vico(122P) and latitude variations of plasma phenomena. *Planet. Space Sci.* **45**, 813–819.

Burton, M. E., N. U. Crooker, G. L. Siscoe, and E. J. Smith 1994. A test of source-surface model predictions of heliospheric current sheet inclination. *J. Geophys. Res.* **99**, 1–9.

Cremonese, G., and M. Fulle 1988. A disconnection event in the ion tail of comet Bradfield 1987s. *Astron. Astrophys.* **202**, L13–L15.

Crooker, N. U., G. L. Siscoe, S. Shodhan, D. F. Webb, J. T. Gosling, and E. J. Smith 1993. Multiple heliospheric current sheets and coronal streamer belt dynamics. *J. Geophys. Res.* **98**, 9371–9381.

Delva, M., K. Schwingenshuh, M. B. Niedner, Jr., and K. I. Gringauz 1991. Comet Halley remote plasma tail observations and in situ solar wind properties: VEGA-1/2 IMF plasma observations and ground-based optical observations from 1 December 1995 to 1 May 1996. *Planet. Space Sci.* **39**, 697–708.

Farnham, T. L., and K. J. Meech 1994. Comparison of the plasma tails of four Comets: P/Halley, Okazaki–Levy–Rudenko, Austin, and Levy. *Astrophys. J. Suppl.* **91**, 419–460.

Hoeksema, J. T. 1991. Large-scale solar and heliospheric magnetic fields. *Adv. Space Res.* **11** (1), 15–(1)24.

Kozuka, Y., T. Saito, S. Numazawa, and T. Takahashi 1991. Dynamical feature of the plasma tail of Comet Levy (1990c). In *Proceedings of the 24th ISAS. Lunar and Planetary Symposium* (H. Mizutani, H. Oya, and M. Shimizu, Eds.), pp. 18–24.

Marsden, R. G., E. J. Smith, J. F. Cooper, and C. Tranquille 1996. *Ulysses* at high heliographic latitudes: An introduction. *Astron. Astrophys.* **316**, 279–286.

McComas, D. J., S. J. Bame, B. L. Barraclough, W. C. Feldman, H. O. Funsten, J. T. Gasling, P. Riley, R. Skoug, A. Balogh, R. Forsyth, B. E. Goldstein, and M. Neugebauer 1998. Ulysses return to the slow solar wind. *Geophys. Res. Lett.* **25**, 1–4.

Niedner, M. B., Jr. 1981. Interplanetary gas. XXVII. A catalogue of disconnection events in cometary plasma tails. *Astophys. J. Suppl.* **46**, 141–157.

Niedner, M. B., Jr. 1982. Interplanetary gas. XXVIII. A study of the three-dimensional properties of interplanetary sector boundaries using disconnection events in cometary plasma tails, *Astrophys. J. Suppl.* **48**, 1–50.

Niedner, M. B., Jr., and J. C. Brandt 1978. Interplanetary gas. XXIII. Plasma tail disconnection events in comets. Evidence for magnetic field line reconnection at interplanetary sector boundaries? *Astrophys. J.* **223**, 655–670.

Niedner, M. B., Jr., and J. C. Brandt 1979. Interplanetary gas. XXIV. Are cometary plasma tail disconnections caused by sector boundary crossings or by encounters with high-speed streams? *Astrophys. J.* **234**, 723–732.

Niedner, M. B., Jr., and K. Schwingenshuh 1987. Plasma-tail activity at the time of the Vega encounters. *Astron. Astrophys.* **187**, 103–108.

Phillips, J. L., S. J. Bame, A. Barnes, B. L. Barraclough, W. C. Feldman, B. E. Goldstein, J. T. Gosling, G. W. Hoogeveen, D. J. McComas, M. Neugebauer, and S. T. Suess 1995a. Ulysses solar wind plasma observations from pole to pole. *Geophys. Res. Lett.* **22**, 3301–3304.

Phillips, J. L., S. J. Bame, W. C. Feldman, B. E. Goldstein, J. T. Gosling, C. M. Hammond, D. J. McComas, M. Neugebauer, E. E. Scime, and S. T. Suess 1995b. Ulysses solar wind plasma observations at high southerly latitudes. *Science* **268**, 1030–1033.

Saito, T., K. Yumoto, K. Hirao, S. Minami, K. Saito, and E. Smith 1987. Structure and dynamics of the plasma tail of Comet P/Halley. I. Knot event on December 31, 1985. *Astron. Astrophys.* **187**, 209–214.

Shultz, R., G. F. O. Schnur, R. M. West, and J. A. Stüwe 1994. A possible disconnection event in the inner coma of Comet Bradfield 1979X. *Planet. Space Sci.* **42**, 635–642.

Smith, E. J., and K.-P. Wenzel 1993. Introduction of the Ulysses encounter with Jupiter. *J. Geophys. Res.* **98**, 21,111–21,127.

Smith, E. J., R. G. Marsden, and D. E. Page 1995. Ulysses above the Sun's south pole: An introduction. *Science* **268**, 1005–1007.

Suess, S. T. 1993. The relationship between coronal and interplanetary magnetic fields. *Adv. Space Res.* **13** (9)31–(9)42.

Suess, S. T., D. J. McComas, S. J. Bame, and B. E. Goldstein 1995. Solar wind eddies and the heliospheric current sheet. *J. Geophys. Res.* **100**, 12,261–12,273.

Voelzke, M. R., and O. T. Matsuura 1998. Morphological analysis of the plasma structures of Comet P/Halley. *Planet. Space Sci.* **46**, 835–841.

Wegmann, R. 1998. Comment on "Global MHD simulation of a comet crossing the HCS" by Yi, Walker, Ogino, and Brandt. *J. Geophys. Res.* **103**, 6633–6635.

Wenzel, K.-P., R. G. Marsden, D. E. Page, and E. J. Smith 1992. The Ulysses mission. *Astron. Astrophys. Suppl. Ser.* **92**, 207–219.

Yi, Y., F. M. Caputo, and J. C. Brandt 1994. Disconnection events (DEs) and sector boundaries. The evidence from Comet Halley 1985–1986. *Planet. Space Sci.* **42**, 705–720.

Yi, Y., R. J. Walker, T. Ogino, and J. C. Brandt 1996. Global magnetohydrodynamic simulation of a comet crossing the heliospheric current sheet. *J. Geophys. Res.* **101**, 27,586–27,601.

Yi, Y., R. J. Walker, T. Ogino, and J. C. Brandt 1998. Reply. *J. Geophys. Res.* **103**, 6637–6639.